The Deepest VLT/FORS2 Spectrum of a $z \sim 7$ Galaxy: An Easy Target for the E-ELT

Eros Vanzella[1]
Adriano Fontana[2]
Laura Pentericci[2]
Marco Castellano[2]
Andrea Grazian[2]
Mauro Giavalisco[3]
Mario Nonino[4]
Stefano Cristiani[4]
Gianni Zamorani[1]
Cristian Vignali[5]

[1] INAF-Osservatorio Astronomico di Bologna, Italy
[2] INAF-Osservatorio Astronomico di Roma, Monteporzio, Italy
[3] Department of Astronomy, University of Massachusetts, Amherst, USA
[4] INAF-Osservatorio Astronomico di Trieste, Italy
[5] Dipartimento di Fisica e Astronomia, Università degli Studi di Bologna, Italy

GDS_1408, a relatively bright (F125W ~ 26 mag), solid $z \sim 7$ galaxy candidate in the Hubble Ultra Deep Field, has been the target of 52 hours of spectroscopic observations with FORS2 at the VLT. This is the deepest spectrum ever obtained for a galaxy at the epoch of reionisation. Neither emission lines nor a continuum were detected up to 10 100 Å, to a limiting equivalent width of 9 Å; a redshift of 6.82 ± 0.1 is determined, combining the superb HST photometry and the deep FORS2 spectrum. This increased redshift accuracy makes ALMA an interesting option for the confirmation of the redshift. The non-detection of Lyman-α in even the best $z \sim 7$ candidate demonstrates the limitations of the current generation of 8–10-metre-class telescopes for these spectroscopic confirmations; future facilities such as JWST and the E-ELT will be necessary to make decisive progress.

The deep panchromatic surveys of the distant Universe with the Hubble Space Telescope (HST), such as the Great Observatories Origins Deep Survey (GOODS), Cosmic Assembly Near-infrared Deep Extragalactic Legacy Survey (CANDELS) and the Hubble Ultra Deep Field (HUDF), have enabled immense progress in identifying candidates for the first galaxies. The redshifts of these targets have been established by photometric redshifts, relying on the cut-off at the Lyman-α break, but spectroscopic confirmation of these redshifts is very challenging. The Lyman-α line is the most prominent emission feature in the optical/near-infrared region (e.g., Vanzella et al., 2011) and is thus seen as a standard for reliable redshift confirmation. Despite immense efforts, only a few objects are spectroscopically confirmed and some of the faint line detections have been proved doubtful when subjected to deeper observations or more elaborate reduction.

However whilst Lyman-α emission is expected in young galaxies, it is a resonant atomic transition which is very sensitive to conditions within the host galaxy, such as the presence of dust and neutral hydrogen, but also to the damping effect of intergalactic neutral H, and particularly the increased neutral H fraction at the end of the reionisation epoch (Miralda-Escudé et al., 2000; Pentericci et al., 2014). For example, Finkelstein et al. (2013) found only one galaxy at $z = 7.51$ out of 43 candidates at $z > 6.5$ with the Keck/MOSFIRE spectrometer and similarly Schenker et al. (2014) found only one possible Lyman-α line at $z = 7.62$ in the their sample of 19 $z \sim 8$ candidates. In addition to the observational difficulties in detecting a faint line in a part of the spectrum strongly affected by spatially and spectrally varying atmospheric transmission, it may be that the emitted Lyman-α is intrinsically weak. Clearly, all these explanations assume that the efficiency of the colour selection based on the Lyman-α break remains extremely high at $z \geq 7$, i.e., that most of current $z \geq 7$ candidates are indeed at their estimated redshifts.

The source HUDF-J033242.56-274656.6 in the HUDF is the brightest (HST F125W = 26.1 ± 0.02 mag) $z \sim 7$ photometric candidate galaxy in this well-studied region. Figure 1 shows the galaxy as it appears in the HST deep optical and near-infrared imaging (HUDF12). The high-redshift nature ($z > 6.5$) is guaranteed by the large observed break between the ultradeep optical and near-infrared bands (Δmag ~ 4 mag) and the well-determined flat behaviour of the spectral energy distribution (SED) in the near-infrared bands, detected with high signal-to-noise ratio (S/N ~ 20–50 with HST's Wide Field Camera 3 [HST-WFC3]). It has been repeatedly selected as a high-redshift candidate from the earliest Near Infrared Camera and Multi-Object Spectrometer (NICMOS) data to the current ultradeep HUDF data over the past ten years (Vanzella et al. [2014a] and references therein), including extensive Very Large Telescope (VLT) spectroscopy with the Focal Reducer/low dispersion Spectrograph (FORS). All these spectra have now been collected and assessed, combining them into an ultradeep spectrum and compared with multi-band photometry (Guo et al., 2013) to derive new insights into the nature of this pivotal target.

FORS2 observations

HUDF-J033242.56-274656.6 galaxy (G2_1408 in Castellano et al. [2010]) has been observed in four different FORS programmes over the period 2009–2012 and data were combined for 084.A0951(A) (Principal Investigator [PI]: A. Fontana), 086.A-0968(A) – 088.A-1013(A) (PI: A. Bunker) and 088.A-1008(A) (PI: R. Bouwens) with exposure times of 18 (Fontana, F18), 27 (Bunker, B27) and 7 (Bouwens, B7) hours on target, for a total usable exposure time of 52 hours. The F18 data were presented in Fontana et al. (2010) who reported a tentative detection of a Lyman-α line at $z = 6.972$. The B27 programme has also been presented in Caruana et al. (2014). Full details of the observations and reduction of the combined observations are given in Vanzella et al. (2014a). The three individual spectra (F18, B27 and B7) and the 52-hour combined one are shown in Figure 2 as S/N images. The combined spectrum is the deepest one of a galaxy at $z \sim 7$ to date.

No Lyman-α emission detected

The available photometry of GDS_1408 already constrains the redshift to be $6.5 < z < 7.0$, thus Lyman-α should occur between observed wavelengths of 9120 and 9730 Å, where FORS2 is an efficient instrument for its detection. Reliable upper limits on the redshift are provided by the clear detections in the z850 band ($z < 7.3$) and the narrowband filter, NB973 ($z < 7$). The FORS2 600z grism

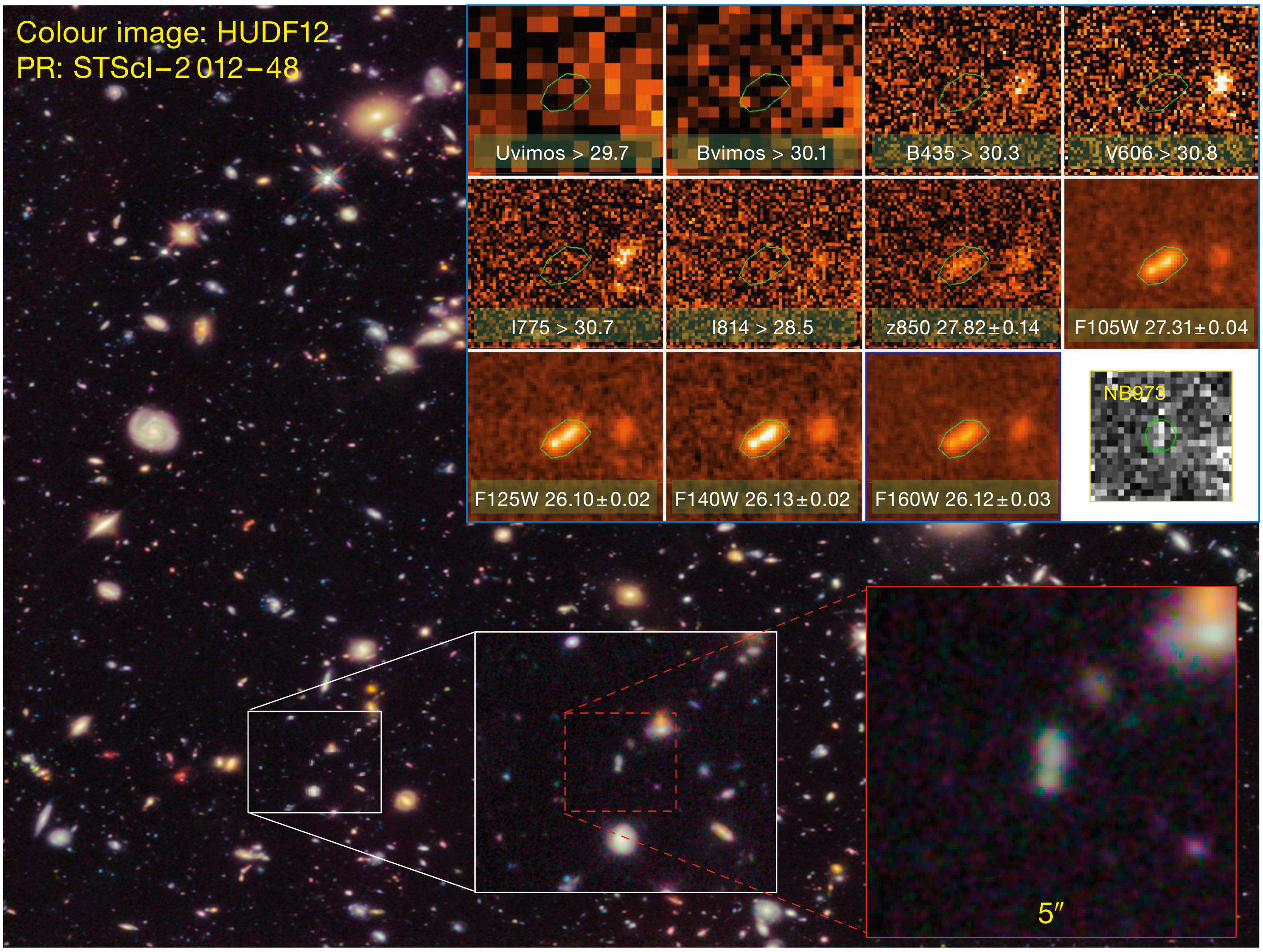

Figure 1. Montage of images of the Hubble Ultra Deep Field focussing on GDS_1408. The background image is from the HST HUDF12 release of Wide Field Camera 3 (WFC3) near-infrared imaging (from STScI Release 2012-48), with enlarged views of GDS_1408 at the bottom. The upper right array of multi-band images (each 3 by 3 arcseconds) shows the appearance of GDS_1408, marked with a green colour, from *U*-band to *H*-band: VIMOS images in *U* and *B*; ACS images in *B*, *V*, *i*, *I* and *z*; WFC3 images in near-infrared bands (filters F105W, F125W [*J*-band], F140W and F160W [*H*-band]); and the detection in the narrowband filter at 973 nm. See Vanzella et al. (2014) for details.

configuration provides a safe constraint on the Lyman-α line flux over the expected range of observed wavelengths. Figure 2 shows that there are no obvious spectral features in the three S/N spectra (F18, B27 and B7) at the position of GDS_1408 (marked by arrows) over the expected wavelength range, indicated by the horizontal dotted line. Most crucially, their combination, shown at the top of Figure 2 shows no emission feature within the expected range, nor a detectable continuum.

The statistical significance of the 52-hour Lyman-α non-detection was estimated by simulations and an upper limit to the Lyman-α flux of 3×10^{-18} erg cm^{-2} s^{-1} at 3–9σ (depending on the exact wavelength position) and its equivalent width (EW) of < 9 Å was determined (see Vanzella et al. [2014a] for details). This represents the faintest limit on the Lyman-α flux ever derived at $z > 6.5$ at such a signal to noise limit.

The depth and photometric quality of data available for this galaxy, and the upper limits derived on the Lyman-α flux and EW, enable the redshift value to be refined by fitting the spectral energy distribution (SED) with young galaxy template spectra and including different equivalent widths for Lyman-α (0–200 Å restframe), focussing on the break between the optical and near-infrared bands. Once the Lyman-α constraints from the spectrum non-detection are included, the redshift of GDS_1408 is constrained between 6.7 and 6.95 at 1σ and 6.6 and 7.1 at 2σ, and produces a refined photometric redshift of 6.82, that is also supported by the broadband Spitzer Infrared Array Camera [IRAC] fluxes (Smit et al. in preparation). The SED fitting has been performed including the full treatment of the nebular emission (both in lines and continuum) and the estimate of the stellar mass is $5^{+3}_{-2} \times 10^9\ M_\odot$, with a dust attenuation E(B - V) ~ 0.1 mag and a dust-corrected star formation rate of $21^{+20}_{-10}\ M_\odot$ yr^{-1} (Vanzella et al. 2014a).

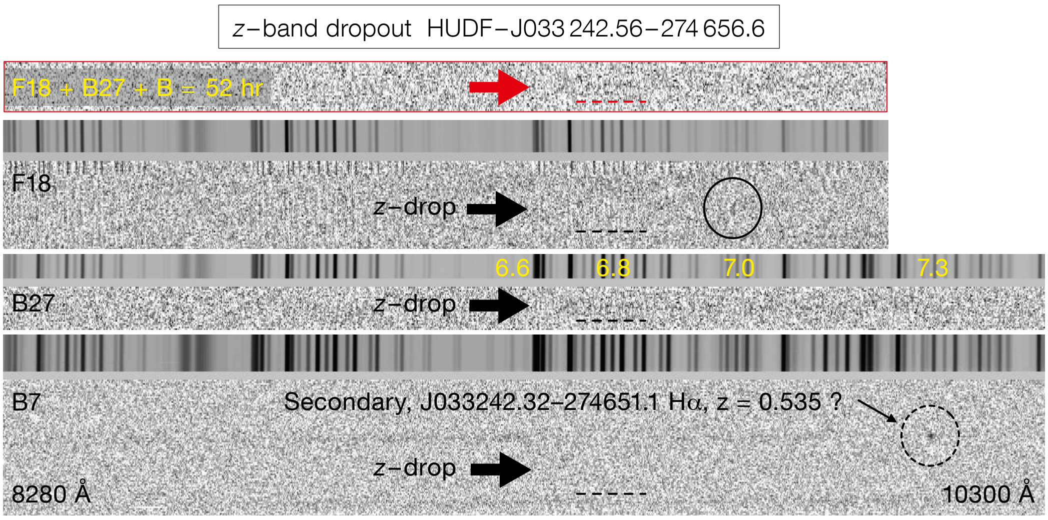

Figure 2. Two-dimensional signal-to-noise spectra and sky spectra of the stacked 52-hour spectrum of the z-band dropout GDS_1408 are shown, with the individual spectra of F18, B27 and B7. The expected position of the Lyman-α continuum break is marked with dotted horizontal lines (see text). In the B27 spectrum the redshift values are reported above the sky as a reference. In the F18 spectrum the dotted circle marks the feature discussed in Fontana et al. (2010). The B7 spectrum shows also the Hα emission from the secondary object J033242.32-274651.1 at z = 0.535, useful here as an example of FORS+600z sensitivity beyond 1 µm. From Vanzella et al. (2014b).

Why no Lyman-α is detected

The combination of excellent photometry and ultradeep spectroscopy point to the conclusion that the extreme weakness of the Ly-α emission is a real feature of GDS_1408. Both the transport of photons out of the galaxy's interstellar medium and the further damping by the intergalactic medium (IGM) can produce a low-surface-brightness Lyman-α glow around galaxies. The escape of Lyman-α photons from a galaxy is a complex process depending on many factors, such as dust and neutral gas, metallicity, gas geometry, etc. (Verhamme et al., 2006). The escaping Lyman-α can be much smaller than the intrinsic Lyman-α luminosity expected from a star formation rate of ~ 20 $M_{\odot}$ yr^{-1}. The neutral H in the IGM will further dampen the Lyman-α emission through scattering. Based on star formation models, an intrinsic flux of the Lyman-α can be derived, implying an upper limit for the effective escape fraction of < 8 % for GDS_1408.

GDS_1408 is one of the more extended sources among the z ~ 7 candidates, with a half-light radius of 0.26 arcseconds, i.e., 1.4 proper kpc (Grazian et al., 2011), and an elongated morphology of 4.8 × 2.5 proper kpc (see Figure 1). It has been shown that the Lyman-α equivalent width and the size observed at 1500 Å in the restframe stellar continuum anticorrelate, such that on average the emitters appear more compact and nucleated than the non-emitters with mean half-light radius of 1 kpc (Law et al., 2007; Vanzella et al., 2009).

Future prospects

The ultradeep FORS2 spectrum demonstrates the current limits of 8–10-metre-class telescopes in the spectroscopic characterisation and redshift measurement of weak Lyman-α emitters at 6.6 < z < 7.3 with 50 hours of on-target exposure. If z ~ 7 is a critical value above which the visibility of Lyman-α lines decreases drastically, then future facilities are necessary to record the spectrum of the ultraviolet (UV) continuum-break and the UV absorption lines and/or optical nebular emission lines from galaxies at 7 < z < 10. The James Webb Space Telescope near-infrared spectrometer (JWST-NIRSPEC) will probe the optical nebular lines ([O II], [O III], [N II] and Balmer series) and the extremely large telescopes (ELT, 30–40-metre diameter) will allow the detection of UV continuum, and absorption lines, down to J ~ 27 mag and the restframe near-infrared emission can be studied by mid-infrared (8–14 µm) instruments, such as the mid-infrared imager-spectrograph (METIS) on the European Extremely Large Telescope (E-ELT).

Before the advent of these facilities, access to z > 6 non-Lyman-α emitters like GDS_1408 or very faint sources (more than ten times fainter than GDS_1408) is feasible only in tiny regions of the sky by relying on the strong gravitational lensing effect provided by galaxy clusters. Spectroscopic observations of feeble galaxies with an intrinsic ultraviolet magnitude as faint as m (1500 Å) ~ 29 have confirmed their ages within the first Gyr after the Big Bang, as recently reported in, e.g., Vanzella et al. (2014b).

Another promising facility that could determine the spectroscopic redshift of GDS_1408, and higher redshift and fainter analogues, is the Atacama Large Millimeter/submillimeter Array (ALMA; e.g., Inoue et al., 2014). The range of probable redshifts for GDS_1408 could be probed by the [C II] 158 µm line, which is observed by ALMA in high-redshift starburst galaxies (e.g., de Breuck et al., 2014). At z > 6.5 the rotational transitions of CO J = 7-6 and J = 6-5 are also observable with ALMA.

References

de Breuck, C. et al. 2014, The Messenger, 156, 38
Caruana, J. et al. 2014, MNRAS, in press, arXiv/1311.0057
Castellano, M. et al. 2010, A&A, 511, 20
Fontana, A. et al. 2010, ApJ, 725, L205
Finkelstein, S. L. et al. 2013, Nature, 502, 524
Grazian, A. et al. 2011, A&A, 532, 33G
Guo, Y. et al. 2013, ApJ, 207, 24
Inoue, A. et al. 2014, ApJ, 780, 18
Law, D. R. et al. 2007, ApJ, 656, 1
Miralda-Escudé, J., Haehnelt, M. & Rees, M. J. 2000, ApJ, 530, 1
Pentericci, L. et al. 2014, arXiv:1403.5466
Schenker, M. A. et al. 2014, arXiv:1404.4632
Vanzella, E. et al. 2009, ApJ, 695, 1163
Vanzella, E. et al. 2011, ApJ, 730, 35
Vanzella, E. et al. 2014a, ApJ, 783, 12
Vanzella, E. et al. 2014b, A&A, in press
Verhamme, A. et al. 2008, A&A, 491, 89